

See discussions, stats, and author profiles for this publication at: <https://www.researchgate.net/publication/231637878>

# Ion Emission from Water Ice Due to Energetic Particle Bombardment†

ARTICLE *in* THE JOURNAL OF PHYSICAL CHEMISTRY A · FEBRUARY 2004

Impact Factor: 2.69 · DOI: 10.1021/jp0373696

---

CITATIONS

19

---

READS

10

5 AUTHORS, INCLUDING:



[Igor Wojciechowski](#)

Alderson-Broadbush College

33 PUBLICATIONS 352 CITATIONS

SEE PROFILE



[Barbara Garrison](#)

Pennsylvania State University

368 PUBLICATIONS 9,271 CITATIONS

SEE PROFILE

Ion Emission from Water Ice Due to Energetic Particle Bombardment<sup>†</sup>Igor A. Wojciechowski,<sup>‡</sup> Shixin Sun,<sup>‡,§</sup> Christopher Szakal,<sup>‡,§</sup> Nicholas Winograd,<sup>‡,§</sup> and Barbara J. Garrison<sup>\*,‡</sup>*Department of Chemistry, 152 Davey Laboratory, Materials Research Institute, 184 MRI Building, Penn State University, University Park, Pennsylvania 16802**Received: November 5, 2003; In Final Form: December 20, 2003*

Ion emission from water ice due to energetic particle bombardment is investigated in a combined molecular dynamics and tof-SIMS experimental study. Specifically, emission of water clusters  $A^\pm(H_2O)_n$ , where  $A^\pm$  denotes positive alkali metal ions,  $Li^+$ ,  $Na^+$ ,  $K^+$ ,  $Cs^+$  or negative halogen ions,  $F^-$ ,  $Cl^-$ ,  $I^-$ , from frozen ice films is investigated. In the experiments, different concentrations of NaI and KI salts were dissolved in water before freezing. The influence of ion charge and concentration is investigated. Cationic clusters eject more effectively than anionic clusters in both the simulations and experiments. Although in most cases the increase of the salt concentration results in a higher absolute ion yield, this dependence is rather complex and is discussed in terms of ion pairing and clustering in the original solution and during emission.

## 1. Introduction

Ion emission from condensed phases under nonequilibrium conditions is important in a number of desorption techniques including secondary ion mass spectrometry (SIMS),<sup>1</sup> matrix-assisted laser desorption/ionization (MALDI),<sup>2</sup> and electrospray ionization.<sup>3</sup> For the special matrix of water ice, the formation mechanism and structure of ionic water clusters is of interest to many researchers.<sup>4</sup> Ion emission from frozen samples bombarded by energetic ions is a commonly considered method for production of cluster ions of volatile liquids.<sup>5</sup> The energetic particle bombardment of Na in ice is the basis for explaining the appearance of an excess of Na in the atmosphere of Europa, a satellite of Jupiter.<sup>6</sup>

Here we consider the ion emission process due to energetic particle bombardment as in SIMS experiments. Although some studies of ion emission were performed two decades ago on relatively simple systems,<sup>7,8</sup> no systematic efforts have been made to understand ionization in organic and biological systems. There are many stages in the bombardment event that can conceivably control the ultimate emission of ions. Namely, ions can be preformed in the original sample,<sup>9</sup> energetic collisions or electronic processes can create ions, ions can then be neutralized as they depart the substrate and, of course, the ion stability is important. The influence of the matrix structure and the interactions among the ion and matrix molecules in the original sample on the emission dynamics is unknown. The challenges of tackling the ionization problem either experimentally or theoretically are daunting.

This study presents the initial step of the detailed theoretical and experimental investigation of ionization in molecular

systems. We consider attachment of ions already present in the sample to parent molecules. This mechanism appears to be a universal way of forming secondary ions, almost independent of the molecule being investigated.<sup>10</sup> The parent molecules can associate with ions of both charges, positive ions such as  $Na^+$ ,  $K^+$ ,  $Cs^+$ , or  $Ag^+$ , and negative ions such as  $F^-$ ,  $Cl^-$ ,  $I^-$ , or  $Au^-$ . It has been proposed that an increase of ion concentration in the sample solution can promote the yields of charged components.<sup>11</sup> This connection, however, is not straightforward because the probability for an ion to emit and to be attached to the molecule(s) is determined by complex movement of ions in the collision cascade region and recombination of oppositely charged ions, thus reducing the number of emitted ions. We start our investigation of ionization with this study of the movement of simple ions in a molecular system to answer the question of how readily these ions eject and attach to the parent molecules. The influence of ion charge and concentration on the ion yield has not been systematically studied to the best of our knowledge.

As a realistic model system for theoretical and experimental studies, water ice has been chosen for investigation. This material is an important matrix for SIMS experiments on frozen-hydrated biological cells.<sup>12</sup> Ions of the type  $(H_3O)^+(H_2O)_n$ ,  $(H_2O)^+(H_2O)_n$ , and  $OH^-(H_2O)_n$  are observed<sup>12–14</sup> although the intensity and cluster size distribution defy simple patterns. Preformed ions can be made by adding simple salts, in which case the mass spectra exhibit peaks corresponding to clusters such as  $Na^+(H_2O)_n$ . These ions probably form by a mechanism similar to the ions observed for organic and biological samples, thus we believe that the water ice system is a good model system for the investigations.

Here we employ the molecular dynamics (MD) method to study the mechanism of attachment of simple cations or anions to water molecules ejected from an ice matrix. This approach has been shown to be effective in describing the motion of the atoms in energetic particle bombardment experiments.<sup>15</sup> Interac-

<sup>†</sup> Part of the special issue "Fritz Schaefer Festschrift".

<sup>\*</sup> Corresponding author. Tel.: +1-814-863-2103. Fax: +1-814-863-5319. E-mail: bjg@psu.edu.

<sup>‡</sup> Department of Chemistry.

<sup>§</sup> Materials Research Institute.

tion potentials for water and ions with water, an essential input to the MD approach, are well established.<sup>16</sup> The ultimate goal is to include quantum mechanical effects into the MD approach to describe motion of hydronium ions<sup>17,18</sup> and hydroxyl ions,<sup>19</sup> collisional ionization of water molecules, and dissociation of neutral water molecules into ion pairs by collision in order to elucidate a comprehensive picture of ionization events during energetic collision cascades.

Specifically, in this initial work molecular dynamics calculations were performed to describe the emission of ionic water clusters  $A^\pm(H_2O)_n$ , where  $A^\pm$  denotes positive or negative ions,  $Li^+$ ,  $Na^+$ ,  $Cs^+$ ,  $F^-$ ,  $Cl^-$ , and  $I^-$ , from an ice film, deposited on a  $Au\{111\}$  surface, under bombardment by 300 eV Ar atoms. An amorphous ice film with a single ion within 2–3 layers of the surface as well as a sample with eight  $Na^+$  and  $Cl^-$  ions were explored in the calculations. To complement the MD simulations, experiments were performed on a water film with dissolved NaI and KI salts of different concentrations. The films were frozen on a silver substrate and then were exposed to a beam of 20 keV  $C_{60}^+$  ions.

Different solvation structures of cations and anions in water are shown to lead to larger absolute yield of cationic  $A^+(H_2O)_n$  clusters as compared to anionic  $A^-(H_2O)_n$  clusters. This finding is supported by related experimental data. An effect of salt concentration in the original sample on the experimental ion yield is discussed in terms of ion pairing and clustering in concentrated solutions.

## 2. MD Simulations

The system investigated is a film of water ice adsorbed on a  $Au\{111\}$  substrate. The metal substrate is included in order to assist in confining the projectile energy in the surface region and reflecting this energy toward the vacuum.<sup>20, 21</sup> All details of the  $H_2O-H_2O$ ,  $H_2O-Au$ , and  $Au-Au$  interaction potentials including the potential parameters have been described earlier.<sup>22</sup> Briefly, to model the water–water interaction, a rigid version of the extended simple-point-charge (SPC/E) water model was used.<sup>23</sup> For the  $Au-H_2O$  interaction, a potential developed previously was applied.<sup>24</sup> The gold substrate was represented by a many-body MD/Monte Carlo corrected effective medium potential function.<sup>25</sup> Halide and alkali ion interactions with water were treated classically. The ions were represented by a point charge having a Lennard-Jones center on it.<sup>26</sup> Ion–ion interactions used in calculations of the concentrated NaCl solution were described by the Huggins-Mayer potential for the non-Coulombic part of the interaction

$$U(r) = A \exp(-Br) - \frac{C}{r^6} \quad (1)$$

with parameters taken from the literature.<sup>27</sup>

In the majority of calculations, the target included an amorphous ice film at 77 K consisting of 1056 water molecules with one ion near the surface, representing infinite dilution. A total of 8  $Na^+$  and 8  $Cl^-$  ions were incorporated for the 1 M NaCl calculation. The water film was placed on the  $\{111\}$  surface of a 9-layer crystallite of 1980 Au atoms. No periodic boundary conditions were applied during the calculation of ion emission.

Since as a first step, only the formation of hydrated alkali and halide cluster ions are considered, we have assumed that the water molecules are not dissociated during the collision cascade. The constraint technique RATTLE<sup>28</sup> and the velocity Verlet algorithm, implemented into the MD code as described

previously,<sup>22,28</sup> were used to maintain fixed O–H bond lengths in the water molecules as well as a fixed H–O–H bond angle. To be consistent with the assumption of nondissociating water molecules, a low energy, 300 eV, for the incident primary Ar particle has been employed. The Ar particle is aimed along the surface normal within a rectangular area ( $\sim 65 \text{ \AA}^2$ ) around the ion for the given set of trials. For each ion, 450 trajectories were performed. Each trajectory lasted for more than 7 ps, sufficient time for the sputter yield to reach a constant value. All emitted clusters, however, were monitored over the next 250 ps to allow the clusters to undergo unimolecular decomposition.

The protocol for heating/cooling the system has been described.<sup>22</sup> To prepare the sample, 12 layers of a hexagonal ice were placed on the metal surface. The system was heated to 300 K and equilibrated over 50 ps at this temperature. An ion was then placed on top of the film. Following a 20 ps equilibration at 300 K, the system with the ion was cooled to 77 K. After this procedure, the ion remained within 2–3 layers of the ice surface. For preparation of the 1 M solution of NaCl, 8 ion pairs were added to the ice. The system was equilibrated over 100 ps at 300 K followed by a fast cooling to 77 K. Periodic boundary conditions in the directions parallel to the surface were applied for all sample preparation procedures.

## 3. Experimental Section

Positive and negative SIMS spectra were acquired with a ToF SIMS apparatus described in detail elsewhere.<sup>29</sup> The samples were prepared by taking 2  $\mu\text{L}$  of each salt solution and spreading them onto individual silver substrates. The sample and substrate were quickly immersed into liquid nitrogen while affixed to a copper sample block. The sample was transferred to the analysis chamber and loaded onto a sample stage cooled with liquid nitrogen to maintain a frozen sample. Samples of NaI and KI were investigated at 0.0001 M, 0.01 M, and 1 M concentrations. Table salt, NaCl, could not be investigated due to isotopic interferences at the mass of  $Cl^-$  with  $OH^-(H_2O)$ . The samples were placed in the spectrometer at the same time and the data were taken on the same day. The analysis chamber has been modified slightly to accommodate the fitting of both  $Ga^+$  and  $C_{60}^+$  ion sources.<sup>30</sup> In principle, to compare quantitatively with the calculations, the experiments should be performed with the  $Ga^+$  ion source with low incident energies. The  $Ga^+$  source, however, caused considerable sample charging and reliable spectra could not be obtained. The use of an electron flood gun does not solve this problem. The  $C_{60}^+$  beam does not produce as much surface charging as atomic projectiles because it seems to result in a more electrically balanced surface after  $C_{60}^+$  bombardment in comparison to the atomic projectile bombardment. Thus, the  $C_{60}^+$  ion source<sup>30</sup> with 20 keV kinetic energy was used. A total time of 10 to 20 s of primary beam at 0.6 nA dc current was needed to remove a water overlayer acquired from the sample transfer, and to expose a fresh surface for analysis.<sup>31</sup> Charge compensation using low-energy electrons was needed to detect signal for negative SIMS spectra. Although the nature of the collision cascades generated by low-energy atomic beams and high-energy  $C_{60}^+$  beams are qualitatively different,<sup>32</sup> we present arguments below that the observed ion signals are strongly influenced by the ion–water interaction. Hence it is the structure of the solid rather than the specifics of the dynamics of the collision cascade that lead to the observable cluster yields.

**TABLE 1: Number of Ionic Water Clusters Ejected in 450 Trajectories of 300 eV Ar Atoms Bombarding the Ice Water Film with One Ion (The counts include bare ions as well as water solvated ions.)**

ions	total number of sputtered ions
Li <sup>+</sup>	97
Na <sup>+</sup>	95
Cs <sup>+</sup>	83
F <sup>-</sup>	18
Cl <sup>-</sup>	8
I <sup>-</sup>	16

#### 4. Results and Discussion

The general trend found in the calculations, more effective emission of cations versus anions, is first discussed in terms of the ion solvation structures in water. The experimental results corroborate this finding. Ion pairing and clustering in the original mixture and during atomic bombardment is proposed to be responsible for a much slower than linear increase in ion yield as a function of salt concentration as well as for the effective emission of bare ions from concentrated solutions as observed in the experimental data.

**4.1. Cation vs Anion Effect.** The total numbers of ionic clusters emitted from the infinite dilution samples by 300 eV Ar projectiles are given in Table 1. The main observation is that cationic water clusters are emitted more effectively than the anionic water clusters. The mass distributions of cationic clusters extend to clusters with 17 water molecules as shown in Figure 1. In contrast, a simulation of bombardment of a Ag surface that results in a similar total yield,<sup>32</sup> on average 17 Ag atoms versus our average 26 water molecules, gives a maximum cluster size of Ag<sub>5</sub>. Presumably, the larger cluster range for solvated ions rather than metal clusters is due to the long ranged ion–dipole and dipole–dipole interactions in the ion–water system.

The more effective emission of cation water clusters as compared to anion clusters can be explained by the different solvation structure of positive and negative ions in water. Both MD and ab-initio calculations of the ion solvation structure in bulk water and at the liquid–vapor interface indicate that cations interact strongly with neighboring water molecules via cation–oxygen attraction, while the interaction of an anion with nearest water molecules is weaker.<sup>33,34</sup> The cation–oxygen interaction results in reorientation of water dipoles in the vicinity of the ion, thus disrupting the hydrogen bond network. Consequently, the local structure can be characterized as an almost preformed solvated ion with weak bonding to the remaining liquid. The preferred orientation of water molecules around a central anion, however, is similar to the orientation around a central water molecule, i.e., the anion in water does not introduce a large perturbation and the hydrogen bond network retains its structural identity near the anion.<sup>34</sup> The net effect is that even though the interaction of the anion with water is locally weaker than the cation with water, the interaction of the anion and its solvation structure with the whole medium is stronger than that for cations.

This feature of the ion–water interactions is illustrated in Figure 2, where the interaction of the sphere of a given radius including the sodium or chlorine ion in the center and surrounding water molecules with the rest of the water molecules is calculated as a function of the radius. The ion position is 2–3 Å below the water surface. The symbols for the smallest radii correspond to the interaction of the bare ion with water. The next radius corresponds to the first solvation shell of water molecules around the Na<sup>+</sup> or Cl<sup>-</sup> ion. The interaction energy

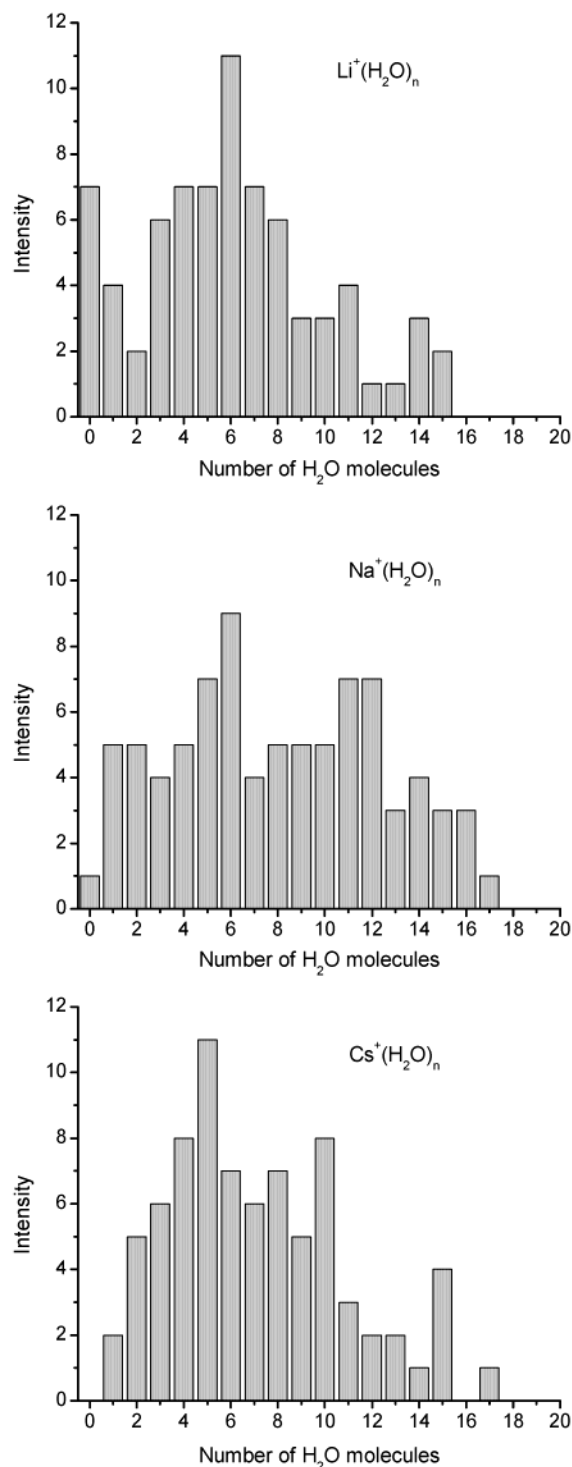


**Figure 1.** Calculated size distributions of cation–water clusters for 300 eV Ar bombardment of the ice film with one ion near the surface of the film. The number of trajectories performed for each ion, Li<sup>+</sup>, Na<sup>+</sup>, and Cs<sup>+</sup>, was 450.

of the Na<sup>+</sup>–water complexes with the remaining system is weaker than that for the Cl<sup>-</sup>–water complexes, while the bare Na<sup>+</sup> is more strongly bonded to the solution than the Cl<sup>-</sup> ion.

Desorption of a cation along with its first solvation shell requires, therefore, less energy than desorption of an anion with its solvation shell. The detailed analysis of sputtering trajectories shows that the water molecules initially adjacent to the cations mainly accompany them in the ejection event. The contribution

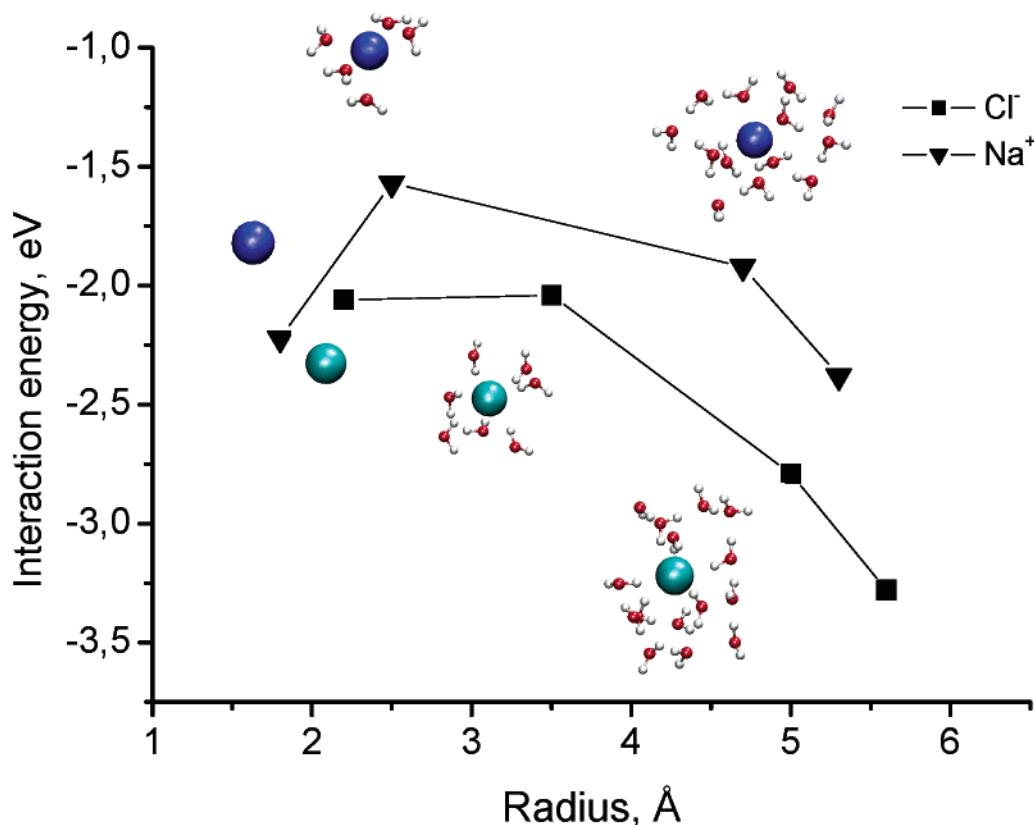


**Figure 2.** The interaction energies of the sphere, with the ion in the center and surrounding waters forming a solvation shell, with the rest of water molecules as a function of the sphere radius.

of bare cations to the ion yield at low concentrations should also be smaller when compared to that of cluster ions.

To check the theoretical findings, the ionic clusters  $A^\pm(H_2O)_n$ , where  $A^\pm$  denotes positive alkali metal ions,  $Na^+$ ,  $K^+$ , or negative halogen ion  $I^-$  were measured in ToF-SIMS experiments. The yields of positive and negative water clusters emitted from the 0.0001 M solution of NaI and KI are presented in Figure 3. Although the yield of Na clusters exceeds the yield of K clusters, emission of positive ions is noticeably more effective than emission of anion-containing clusters, consistent with the theoretical predictions. Spectra similar to those for NaI were also observed for NaBr and CsI solutions at a single concentration.<sup>35</sup> In addition, for both the NaI and KI solutions, the intensities of the  $(H_3O)^+(H_2O)_n$  species are considerably greater than the intensities of the  $OH^-(H_2O)_n$  species<sup>35</sup> although it is not possible to ascertain that the hydronium ions are present (or created) at the same concentration as the hydroxyl ions.

**4.2. Concentration Effect.** The concentration effect, observed in the experiment, is demonstrated in Figure 4 for both cations and anions of NaI and KI. Even though the original salt concentration differs by 2 and 4 orders of magnitude, all the data fit on the same linear scale. The distributions look similar for the 0.0001 and 0.01 M solutions, while the spectra for the 1 M solutions exhibit relatively higher yields of bare ions, such as  $Na^+$ ,  $K^+$ , and  $I^-$ .

The observation of a relatively large number of bare ions for the 1 M solutions relative to the lower concentration solutions is consistent among the various systems studied experimentally. To investigate the concentration effect, we modeled the sputtering of a sample of eight  $Na^+$  and eight  $Cl^-$  ions in the water sample, a concentration that is approximately 1 M. The yields of species ejected are given in Table 2. The most abundant

**TABLE 2: Numbers of Ion-Containing Clusters for 300 Trajectories of 300 eV Ar Atoms Bombarding the 1 M Solution of NaCl (Numbers in the left column,  $n$ ,  $m$ ,  $x$ , indicate how many of  $Na^+$  ( $n$ ),  $Cl^-$  ( $m$ ), and  $H_2O$  ( $x$ ) species are in the emitted clusters.)**

$Na_n^+Cl_m^-(H_2O)_x$	total number of ejected clusters	charge of cluster
1, 0, 0	8	+1
0, 1, 0	3	-1
1, 0, >0	21	+1
0, 1, >0	4	-1
1, 1, $\geq 0$	35	0
1, 2, $\geq 0$	3	-1
2, 1, $\geq 0$	10	+1
2, 2, $\geq 0$	6	0
3, 2, $\geq 0$	2	+1
2, 4, $\geq 0$	1	-2

cluster is the one with one cation and one anion, that is, a neutral species that would not be detected. In total there are 52 charged clusters of which 11 (21%) are bare ions. For the isolated ion calculations, the bare ions only contribute 1–3% to the total yield. Thus, the calculations confirm the experimental finding that there are a relatively large number of bare ions. The mechanistic reason for the large number of bare ions as well as for the deficiency in ion yields for the higher concentrations relates back to the structure of the ionic solutions of the original film.

For 1 M NaCl solutions at room temperature, simulations show quite clearly that there is considerable clustering of ions in the water.<sup>36–40</sup> One prediction at room temperature is that 16% of the total ions are clustered as neutral NaCl dimers, 19% as singly charged trimers, 2% as neutral tetramers, and the remaining 63% of the ions are in similar environments as the



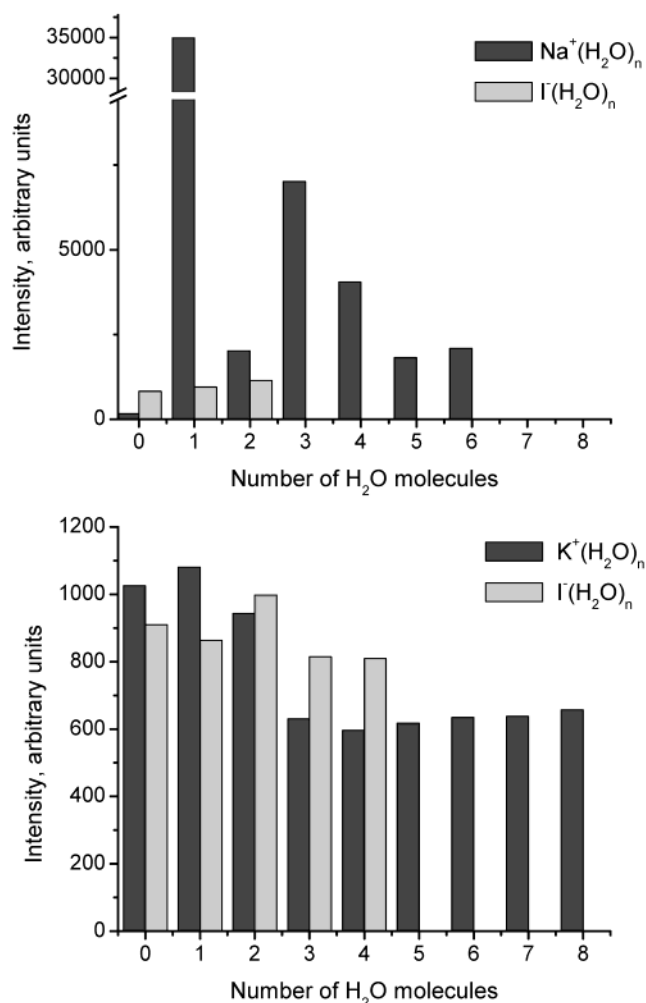


**Figure 3.** Size distributions of cation and anion water clusters obtained experimentally with 20 keV C<sub>60</sub><sup>+</sup> bombardment of water ice with dissolved NaI and KI at 0.0001 M concentration.

dilute solution.<sup>37</sup> According to other data,<sup>38</sup> the concentration of the complexes with two or more ions of the same charge in close vicinity of one another can reach 0.2 M for the 1 M solution. These ion clusters can and do have intervening water molecules but are recognizable as localized entities. As the density of the liquid decreases, a situation that occurs during the particle emission in the bombardment event, the amount of clustering of ions increases because there is less water to stabilize individual solute ions. In opposite charge complexes, the ions form neutral species that cannot be detected. In the like charge complexes, the ions repel each other in the lower density conditions and eject as bare ions.

The above discussion explains the presence of the bare ions at high concentration in terms of the initial film structure and a minimal collision cascade caused by 300 eV Ar bombardment. The C<sub>60</sub><sup>+</sup> bombardment event leads to numerous overlapping collision cascades that create a highly disordered region in a short time leading to a dense liquidlike region.<sup>32</sup> These motions should further enhance pairing of opposite-charged species and repulsion of like-charged species. Thus, at high concentrations, the number of ions that reach the detector is not proportional to the initial concentration in the film. A concentration effect has also been observed in studies of laser-irradiated aerosol particles.<sup>41</sup> These authors observe that the ion signal is linear in concentration of ions up to a little over 0.0001 M and then saturates as the concentration approaches 1 M. They interpret

the saturation of the ion signal as being caused by ions of opposite charge associating under high-temperature conditions.

To evaluate properly the ion yield at low concentration in the simulation, we should perform calculations with a large sample with multiple ions incorporated at the concentration of interest. It is possible, however, to estimate a value. The 65 Å<sup>2</sup> bombardment zone, if extended 8 Å deep into the surface, corresponds approximately to 0.0001 M. For the isolated ion simulations, >20% of the incident particles give rise to an ejected ion (Table 1). The total ion yield at high concentration (Table 2) is approximately 16%. Thus, the simulations are consistent with the experimental observation that the ion yield is not proportional to concentration.

**4.3. Features Not Understood.** Some features remain unclear in terms of this simple model. Although no mass effect was found in the calculations, the overall positive ion signals for NaI and KI series of low concentration differ by more than an order of magnitude. We also do not understand which factors control the maximum cluster size in both positive and negative series. The maximal cluster size, observed in the experiment, is limited to 6–8 water molecules, while the calculated spectra extend to 15–18 water molecules.

## 5. Conclusions

This combined calculation and experimental study of the ejection of preformed ions in keV particle bombardment has elucidated several important features of the emission process. First, we observe significantly more cations than anions in the spectra for the low initial concentrations of ions. Moreover, a distribution of solvated cation clusters extends to 17 water molecules. From a microscopic viewpoint, the anions do not disrupt the hydrogen bond network in the water, thus the anions are trapped inside the matrix and do not readily eject. The cations, on the other hand, establish a preformed complex that breaks down the hydrogen-bonded network, thus allowing the cluster to eject more easily. The concept that ions (or other species) can destabilize the original matrix and thus alter the ejection properties in SIMS experiments is new and has potential general applicability to other matrixes besides water ice.

We observe that the initial distribution of ions in the solution influences the yield at high concentrations. The original solution has regions of ions of opposite charge in close proximity. These ions tend to neutralize each other, thus the yield of detected ions is not proportional to the initial concentration. There are also configurations of nearby ions of the same charge. These configurations are destabilized during the bombardment event and bare ions tend to be ejected. Certainly, there can be association of ions of opposite charges during the sputtering event, especially with the C<sub>60</sub> bombardment at 20 keV. It is also conceivable that the bombardment event causes ions of like charges to interact and repel each other. Although these dynamic events can be important, the pairing of ions of opposite and like charges in the initial film can explain the major features of the concentration effect. Neutralization of charges of opposite sign should be ubiquitous in all SIMS experiments with preformed ions.

The major ions observed in the experimental spectrum are the clusters associated with hydronium, hydroxyl, and water ions. The initial hydronium and hydroxyl ion concentrations are presumably around 10<sup>-7</sup> M with the water ion, H<sub>2</sub>O<sup>+</sup>, concentration even lower. To account for these high observed signals, the water ions must be formed during the collision cascade. The next step in our modeling studies will be to include collision-induced ionization events.

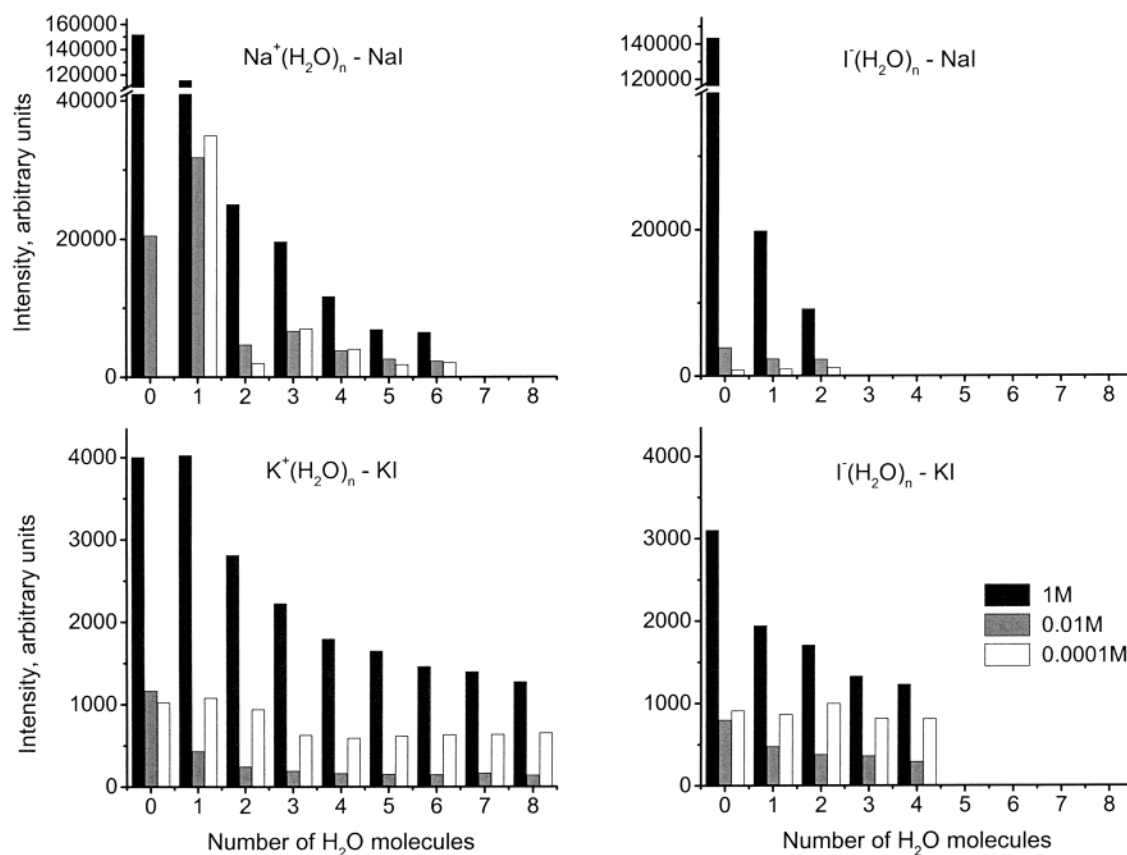


**Figure 4.** Size distributions of ionic water clusters for cations and anions at 0.0001 M, 0.01 M, and 1 M salt concentrations obtained experimentally with 20 keV  $C_{60}^+$  bombardment of ice with dissolved NaI and KI.

**Acknowledgment.** The work was supported by the National Science Foundation through the Chemistry Division and National Institute of Health. The computational support was provided by Academic Services and Emerging Technologies (ASET) group at Penn State University.

## References and Notes

- (1) See, for example, *ToF-SIMS: Surface Analysis by Mass Spectrometry*; Vickerman, J. C., Briggs, D., Eds.; IM Publications and Surface Spectra Limited: Manchester and Chichester, 2001.
- (2) See, for example, Hillenkamp, F.; Karas, M.; Beavis, R. C.; Chait, B. T. *Anal. Chem.*, **1991**, *63*, 1193A.
- (3) See, for example, Whitehouse, C. A.; Dreyer, R. N.; Yamashita, M.; Fenn, J. B. *Anal. Chem.*, **1985**, *57*, 675.
- (4) Zhou, J.; Lu, X.; Wang, Y.; Shi, J. *Fluid Phase Equilibria* **2002**, *194–197*, 257.
- (5) Boryak, O. A.; Stepanov, I. O.; Kosevich, M. V.; Shelkovsky, V. S.; Orlov, V. V.; Blagoy, Yu. P. *Eur. Mass Spectrom.* **1996**, *2*, 329.
- (6) Johnson, R. E. *Icarus* **2000**, *143*, 429.
- (7) Williams, P. *Surf. Sci.* **1979**, *90*, 588.
- (8) Yu, M. L.; Lang, N. D. *Nucl. Instrum. Methods Phys. Res. B* **1986**, *14*, 403.
- (9) Pachuta, S. J.; Cooks, R. G. *Chem. Rev.* **1987**, *87*, 647.
- (10) Hagenhoff, B. In *ToF-SIMS: Surface Analysis by Mass Spectrometry*; Vickerman, J. C., Briggs, D., Eds.; IM Publications and Surface Spectra Limited: Manchester and Chichester, 2001; p 285.
- (11) Gusev, A. I.; Choi, B. K.; Hercules, D. M. *J. Mass Spectrom.* **1998**, *33*, 480.
- (12) Roddy, T. P.; Cannon, D. M., Jr.; Meserole, C. A.; Winograd, N.; Ewing, A. G. *Anal. Chem.* **2002**, *74*, 4011.
- (13) Lancaster, G. M.; Honda, F.; Fukuda, Y.; Rabalais, J. W. *J. Am. Chem. Soc.* **1979**, *101*, 1951.
- (14) Donsig, H. A.; Vickerman, J. C. *J. Chem. Soc., Faraday* **1998**, *93*, 2755.
- (15) Garrison, B. J., In *ToF-SIMS: Surface Analysis by Mass Spectrometry*; Vickerman, J. C., Briggs, D., Eds.; IM Publications and Surface Spectra Limited: Manchester and Chichester, 2001; p 223.
- (16) Koneshan, S.; Rasaiah, J. C.; Dang, L. X.; *J. Chem. Phys.* **2001**, *114*, 7544.
- (17) Von Grotthuss, C. *Ann. Chim.* **1806**, *LVII*, 54.
- (18) Schmitt, U. W.; Voth, G. A. *J. Phys. Chem. B* **1998**, *102*, 5547.
- (19) Chen, B.; Ivanov, I.; Park, J. M.; Parrinello, M.; Klein, M. L. *J. Chem. Phys. B* **2002**, *106*, 12006.
- (20) Delcorte, A.; Vanden Eynde, X.; Bertrand, P.; Vickerman, J. C.; Garrison, B. J. *J. Phys. Chem. B* **2000**, *104*, 2673.
- (21) Delcorte, A.; Garrison, B. J. *J. Phys. Chem. B* **2000**, *104*, 6785.
- (22) Dou, Y.; Zhigilei, L. V.; Winograd, N.; Garrison, B. J. *J. Phys. Chem. A* **2001**, *105*, 2748.
- (23) Berendsen, H. J. C.; Postma, J. P. M.; van Gunsteren, V. F.; Hermans, J. In *Intermolecular forces*; Pullman, B., Ed.; Reidel: Dordrecht, 1981.
- (24) Spohr, E. *J. Mol. Liq.* **1995**, *64*, 91.
- (25) Kelchkar, C. L.; Halsted, D. M.; Perkins, L. S.; DePristo, N. M. *A. E. Surf. Sci.*, **1994**, *310*, 425.
- (26) Lee, S. H.; Rasaiah, J. C. *J. Phys. Chem.* **1996**, *100*, 1420.
- (27) Pettit, B. M.; Rossky, P. J. *J. Chem. Phys.* **1986**, *84*, 5836.
- (28) Andersen, H. C. *J. Comput. Phys.* **1983**, *52*, 24.
- (29) Braun, R. M.; Blenkinsopp, P.; Mullock, S. J.; Corlett, C.; Willey, K. F.; Vickerman, J. C.; Winograd, N. *Rapid Commun. Mass Spectrosc.* **1998**, *12*, 1246.
- (30) Weibel, D.; Wong, S.; Lockyer, N.; Blenkinsopp, P.; Hill, R.; Vickerman, J. C. *Anal. Chem.* **2003**, *75*, 1754.
- (31) Wucher, A.; Sun, S.; Szakal, C.; Winograd, N. Molecular Sputter Depth Profiling in Ice Matrixes Using  $C_{60}$  Projectiles. *Appl. Surf. Sci.*, in press.
- (32) Postawa, Z.; Czerwinski, B.; Szewczyk, M.; Smiley, E. J.; Winograd, N.; Garrison, B. J. *Anal. Chem.* **2003**, *75*, 4402.
- (33) Dang, L. X. *J. Phys. Chem. B* **2002**, *106*, 10388.
- (34) Ayala, R.; Martínez, J. M.; Pappalardo, R. R.; Marcos, E. S. *J. Phys. Chem. A* **2000**, *104*, 2799.
- (35) Sun, S.; Szakal, C.; Winograd, N. Unpublished.
- (36) Oelkers, E. H.; Helgeson, H. C. *Science* **1993**, *261*, 888.
- (37) Driesner, T.; Seward, T. M.; Tironi, I. G. *Geochim. Cosmochim. Acta* **1998**, *62*, 3095.
- (38) Degève, L.; da Silva, F. L. B. *J. Mol. Liq.* **2000**, *87*, 217.
- (39) Sherman, D. M.; Collings, M. D. *Geochem. Trans.* **2002**, *3*, 102.
- (40) Chialvo, A. A.; Cummings, P. T.; Simonson, J. M.; Mesmer, R. E. *J. Mol. Liq.* **1997**, *73–74*, 361.
- (41) Dessiaterik, Yu.; Nguyen, T.; Baer, T.; Miller, R. *J. Phys. Chem.*, submitted